JACS
JOURNAL OF THE AMERICAN CHEMICAL SOCIETY
Article
pubs.acs.org/JACS

Mechanisms of the Thermal and Catalytic Redistributions, Oligomerizations, and Polymerizations of Linear Diborazanes

Alasdair P. M. Robertson,[†] Erin M. Leitao,[†] Titel Jurca,[†] Mairi F. Haddow,[†] Holger Helten,*[,‡] Guy C. Lloyd-Jones,*[,†] and Ian Manners*[,†]

[†]School of Chemistry, University of Bristol, Cantock's Close, Bristol BS8 1TS, United Kingdom
[‡]Institute of Inorganic Chemistry, RWTH Aachen University, Landoltweg 1, 52056 Aachen, Germany

Supporting Information

ABSTRACT: Linear diborazanes $R_3N{-}BH_2{-}NR_2{-}BH_3$ (R = alkyl or H) are often implicated as key intermediates in the dehydrocoupling/dehydrogenation of amine-boranes to form oligo- and polyaminoboranes. Here we report detailed studies of the reactivity of three related examples: $Me_3N{-}BH_2{-}NMe_2{-}BH_3$ (**1**), $Me_3N{-}BH_2{-}NHMe{-}BH_3$ (**2**), and $MeNH_2{-}BH_2{-}NHMe{-}BH_3$ (**3**). The mechanisms of the thermal and catalytic redistributions of **1** were investigated in depth using temporal-concentration studies, deuterium labeling, and DFT calculations. The results indicated that, although the products formed under both thermal and catalytic regimes are identical ($Me_3N{\cdot}BH_3$ (**8**) and $[Me_2N{-}BH_2]_2$ (**9a**)), the mechanisms of their formation differ significantly. The thermal pathway was found to involve the dissociation of the terminal amine to form $[H_2B(\mu\text{-}H)(\mu\text{-}NMe_2)BH_2]$ (**5**) and NMe_3 as intermediates, with the former operating as a catalyst and accelerating the redistribution of **1**. Intermediate **5** was then transformed to amine-borane **8** and the cyclic diborazane **9a** by two different mechanisms. In contrast, under catalytic conditions (0.3−2 mol % IrH_2POCOP (POCOP = κ^3-1,3-$(OPtBu_2)_2C_6H_3$)), **8** was found to inhibit the redistribution of **1** by coordination to the Ir-center. Furthermore, the catalytic pathway involved direct formation of **8** and $Me_2N{=}BH_2$ (**9b**), which spontaneously dimerizes to give **9a**, with the absence of **5** and BH_3 as intermediates. The mechanisms elucidated for **1** are also likely to be applicable to other diborazanes, for example, **2** and **3**, for which detailed mechanistic studies are impaired by complex post-redistribution chemistry. This includes both metal-free and metal-mediated oligomerization of $MeNH{=}BH_2$ (**10**) to form oligoaminoborane $[MeNH{-}BH_2]_x$ (**11**) or polyaminoborane $[MeNH{-}BH_2]_n$ (**16**) following the initial redistribution reaction.

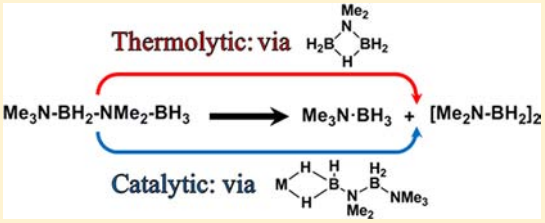

INTRODUCTION

Amine-boranes, $RR'NH{\cdot}BH_3$ (R, R′ = alkyl, aryl or H), are well-known main group compounds that have traditionally found applications as hydroboration and reducing reagents, primarily within organic synthesis.[1−3] Recently however, the development of catalytic dehydrogenation protocols for such species had led to growing interest in their potential uses as hydrogen storage and transfer reagents[4−11] and as precursors to polyaminoboranes, inorganic analogues of polyolefins.[12−15] Amine-boranes are also of interest as precursors to boron nitride materials, including "white graphene", monolayer films of hexagonal boron nitride, through dehydrogenation on Cu surfaces.[16,17]

Of critical importance to the development of amine-boranes as hydrogen storage/transfer materials and polymer precursors is a detailed understanding of the mechanistic aspects of their metal-catalyzed dehydrogenation and dehydrocoupling. Progress in this area has been advanced by a number of experimental and theoretical studies that provide mechanistic insight for a variety of catalyst systems.[13,18−27] Although the exact mechanisms appear to vary with the specific substrate/catalyst combination, a common feature is the implication of monomeric aminoboranes, $R_2N{=}BH_2$, and/or linear diborazanes, $R_2NH{-}BH_2{-}NR_2{-}BH_3$ (R = alkyl or H), as key reactive intermediates.

It is notable that monomeric primary aminoboranes and related secondary aminoboranes with small substituents are elusive as they readily dimerize/oligomerize. Linear diborazanes, on the other hand, are synthetically accessible and can therefore be readily studied. Very little is known about their reactivity but, as noted above, they have been detected in several mechanistic investigations of amine-borane dehydrogenation and dehydrocoupling reactions.[21,26,28−38] For example, in the Cp_2Ti-catalyzed dehydrocoupling of $Me_2NH{\cdot}BH_3$ (**7**), the linear diborazane $Me_2NH{-}BH_2{-}NMe_2{-}BH_3$ is formed which subsequently eliminates H_2 to generate the cyclodiborazane $[Me_2N{-}BH_2]_2$ (**9a**) as the final product (Scheme 1).[19,31] In addition, coordinated diborazanes have also been identified in deprotonated form as intermediates in group 2- and group 3-mediated dehydrocouplings of amine-boranes.[39−41]

The potential mechanistic complexity of dehydrocoupling reactions is also illustrated by the possibility that linear diborazanes may also result from off-metal pathways. For

Received: May 6, 2013
Published: August 13, 2013

   dx.doi.org/10.1021/ja404247r | J. Am. Chem. Soc. 2013, 135, 12670−12683

Scheme 1. Proposed Mechanism of the [Cp_2Ti]-Catalyzed Dehydrocoupling of $Me_2NH{\cdot}BH_3$ (7)[a]

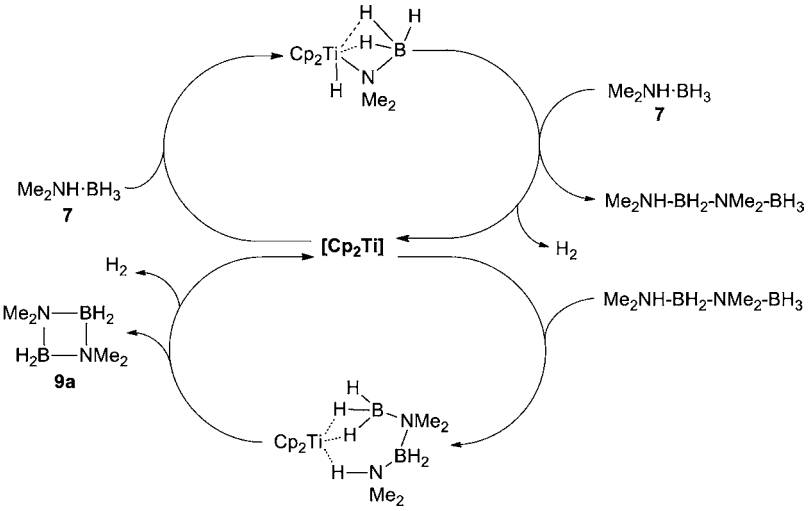

[a]Modified from refs 19 and 31.

example, monomeric aminoboranes, which are also often detected as intermediates in dehydrocoupling reactions, have been proposed to react with residual amine-borane substrate to generate these species (Scheme 2).[21,27]

Scheme 2. Proposed Mechanistic Pathways and Intermediates in the Dehydrocoupling of $Me_2NH{\cdot}BH_3$ (7)[a]

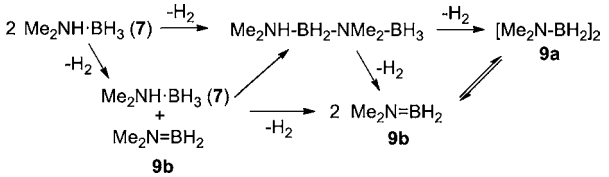

[a]Modified from ref 21.

The linear diborazane $MeNH_2{-}BH_2{-}NHMe{-}BH_3$ (**3**) has also been identified in ligated form by Weller and co-workers as a product of the Ir-mediated oligomerization of $MeNH_2{\cdot}BH_3$ (**6**) (Scheme 3).[36] The same complex of **3** was also shown to be accessible from the direct reaction of **3** with the cationic Ir precursor.

Scheme 3. Model Compound Chemistry of Ir/Amine-Borane Complexes, Postulated to Represent the First Steps in the Polymerization of $MeNH_2{\cdot}BH_3$ (6) to Yield [$MeNH{-}BH_2]_n$ (16) at Ir Centers[a]

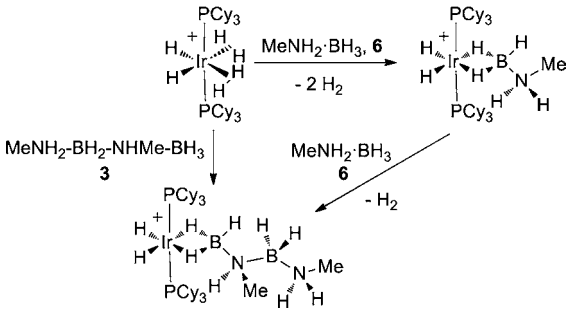

[a]The anion, $[B(3,5\text{-}C_6H_3(CF_3)_2)_4]^-$, associated with Ir centers is not shown.

In addition to catalytic dehydrocyclization, it has been previously demonstrated that, under thermolytic conditions, diborazanes can undergo redistribution reactions to produce an amine-borane and aminoborane pair (Scheme 4).[42] This process is effectively the reverse reaction to the almost thermoneutral ($\Delta G = -2.3$ kcal·mol^{-1}) diborazane formation pathway noted earlier (see Scheme 2).[21,27]

Scheme 4. Thermal Redistribution of $Me_3N{-}BH_2{-}NMe_2{-}BH_3$ (1) as Demonstrated by Burg and Randolph[42]

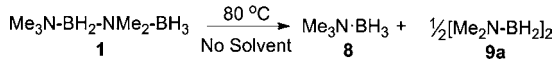

Clearly, detailed studies of a series of linear diborazanes would be expected to provide much needed insight into the role of these species in dehydrocoupling/dehydrogenation reactions. In a recent preliminary communication,[43] we briefly reported the formation of poly(methylaminoborane) [$MeNH{-}BH_2]_n$ (**16**) from $MeNH_2{-}BH_2{-}NHMe{-}BH_3$ (**3**) using 0.3 mol % IrH_2POCOP (POCOP = κ^3-1,3-$(OPtBu_2)_2C_6H_3$) as a catalyst. This was proposed to result from an initial redistribution of the linear diborazane followed by subsequent dehydropolymerization and coordination polymerization of the ensuing amine-borane **6** and aminoborane $MeNH{=}BH_2$ (**10**), respectively. In this paper, we elaborate on our initial results with **3** and also present full details of our studies of two further related linear diborazanes, $MeR_2N{-}BH_2{-}NMeR'{-}BH_3$ (R = R′ = Me (**1**); R = Me, R′ = H (**2**)) with a focus on both the thermal and metal-catalyzed redistributions of these species.

RESULTS AND DISCUSSION

A relatively limited number of linear diborazanes have been previously reported, and these examples were accessed through a variety of synthetic methods.[42,44−47] The most common route to such species has involved the low yielding reaction of lithium amidoboranes, $Li[R_2N{\cdot}BH_3]$, with B-chlorinated amine-boranes, $R_2NH{\cdot}BH_2Cl$.[45] Prior to this, diborazanes had also been accessed via the reaction of amines with μ-amidodiboranes, $[H_2B(\mu\text{-}H)(\mu\text{-}NR_2)BH_2]$, with the first synthesis of this type documented by Burg and co-workers in 1938.[48,49] In this, and

dx.doi.org/10.1021/ja404247r | J. Am. Chem. Soc. 2013, 135, 12670−12683

subsequent preparations, the μ-amidodiboranes were accessed through the reaction of diborane, B_2H_6, and the required amine in the condensed phase. Significantly, this method was recently further developed by Shore and Zhao, who reported the synthesis of the simplest diborazane $NH_3{-}BH_2{-}NH_2{-}BH_3$ via the reaction of NH_3 with $[H_2B(\mu\text{-}H)(\mu\text{-}NH_2)BH_2]$, which was itself prepared from $NH_3{\cdot}BH_3$ and $BH_3{\cdot}THF$ (Scheme 5).[46]

Scheme 5. Synthesis of Linear Diborazane $NH_3{-}BH_2{-}NH_2{-}BH_3$[46]

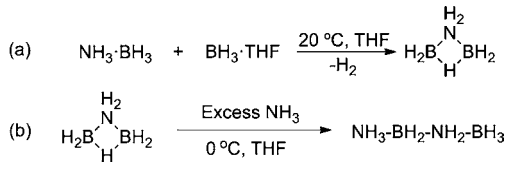

The potential generality of this route, and the circumvention of the use of B_2H_6, inspired us to investigate the synthesis of a range of other new linear diborazanes via this method with a view to probing their chemistry.

1. Synthesis and Characterization of Linear Diborazanes $MeR_2N{-}BH_2{-}NR'Me{-}BH_3$ (R = R′ = Me (1); R = Me, R′ = H (2); R = R′ = H (3)). Syntheses of diborazanes containing internal dimethylamido (**1**) or methylamido (**2** and **3**) moieties were carried out using a modification of the aforementioned method of Shore and Zhao[46] via μ-amidodiborane intermediates $[H_2B(\mu\text{-}H)(\mu\text{-}NR'Me)BH_2]$ (R′ = H (**4**); R = Me (**5**)), respectively. A solution of the amidodiborane was prepared via heating a mixture of either $MeNH_2{\cdot}BH_3$ (**6**) or $Me_2NH{\cdot}BH_3$ (**7**) with $BH_3{\cdot}THF$ in THF at 60 °C over 24−48 h, with subsequent vacuum transfer removing residual amine-borane (Scheme 6a). Analysis of these

Scheme 6. Synthesis of (a) $[H_2B(\mu\text{-}H)(\mu\text{-}NR'Me)BH_2]$ (R′ = H (4); R = Me, (5)) and (b) $MeR_2N\text{-}BH_2{-}NR'Me\text{-}BH_3$ (R = R′ = Me (1); R = Me, R′ = H (2); R = R′ = H (3))

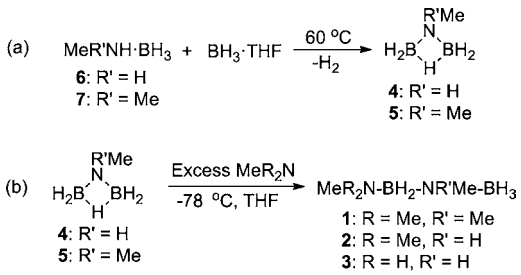

solutions by ^{11}B NMR spectroscopy indicated the presence of a single boron containing product present as a poorly resolved triplet of doublets at −23.2 ppm (**4**) and −18.4 ppm (**5**) consistent with splitting of the boron signals by the terminal and bridging hydride moieties. Amidodiboranes **4** and **5** were then employed in the preparation of $Me_3N{-}BH_2{-}NMe_2{-}BH_3$ (**1**), $Me_3N{-}BH_2{-}NHMe{-}BH_3$ (**2**), and $MeNH_2{-}BH_2{-}NHMe{-}BH_3$ (**3**)[50] through reaction with THF solutions containing ca. 1.1 equiv of Me_3N or $MeNH_2$, respectively (Scheme 6b).

Upon warming to ambient temperature, removal of all volatiles under high vacuum and recrystallization from either THF/hexanes (**1**) or DCM/hexanes (**2** and **3**) yielded colorless crystalline solids for all three linear diborazanes, that each exhibited two signals in the ^{11}B NMR spectrum (in $CDCl_3$) corresponding to the internal and terminal borane moieties, respectively (Table 1). Both the ^1H and ^{13}C NMR spectra of **1**−**3** were unremarkable, but were consistent with the assigned structures.

In the case of $Me_3N{-}BH_2{-}NMe_2{-}BH_3$ (**1**), despite repeated recrystallization, trace amounts of residual amidodiborane **5** remained apparent (*ca.* 4%) by ^{11}B NMR spectroscopy and attempts to produce single crystals suitable for X-ray diffraction were unsuccessful. We postulate that in this case the diborazane may be in equilibrium with free Me_3N and **5**, with **5** also apparent by ^1H NMR spectroscopy (δ_H = 2.60 ppm).[51] Such an observation could be rationalized by an increased degree of steric repulsion between the methyl groups at the two nitrogen centers in this case, which may reduce the strength of the bond to the terminal Me_3N moiety. The presence of an equilibrium between **1** and its precursors was further underlined by the addition of an excess of $MeNH_2$ solution (2 M in THF) to solid **1** at −78 °C. Upon warming to ambient temperature and stirring overnight, quantitative conversion to a novel diborazane, $MeNH_2{-}BH_2{-}NMe_2{-}BH_3$, was observed (see Supporting Information for characterization details), consistent with the presence of a highly labile terminal amine group in diborazane **1**.

Recrystallization of linear diborazanes **2** or **3**[50] from DCM/hexanes at −40 °C produced large colorless crystals suitable for study by single crystal X-ray diffraction, which confirmed the atom connectivity suggested by spectroscopic data. As a result of their similar structures, we show only the molecular structure of **3** (see Figure 1, for the case of **2** see Supporting Information Figure SI-1). Compound **3** crystallized in the monoclinic space group $P2_1/c$, with a single molecule per asymmetric unit. The central B−N chain was found to adopt a gauche conformation, as observed for the related unsubstituted species $NH_3{-}BH_2{-}NH_2{-}BH_3$.[46] The three B−N bonds B1−N1 = 1.5870(10) Å, N2−B1 = 1.5741(9) Å and B2−N2 = 1.5896(9) Å, were consistent with the lengths previously reported for B−N single bonds (Table 2),[45,52] and all nitrogen and boron centers were close to tetrahedral in nature. Molecules of **3** were also found to exhibit short intermolecular B−H−H−N interactions (2.17(1) Å) between hydridic hydrogens at boron (B2) and protic hydrogens at nitrogen (N2), which creates stacks of molecules in the solid state (Figure 1). This is in contrast to the intermolecular dihydrogen bonding reported for the related species $(C_4H_8)NH{-}BH_2{-}N(C_4H_8){-}BH_3$, where the short contacts exclusively involve two separate B−H−H−N inter-

Table 1. ^{11}B NMR Spectroscopic Data Recorded in $CDCl_3$ for Linear Diborazanes 1−3

	^{11}B NMR, $CDCl_3$			
Diborazane	δ internal BH_2/ppm	J_{BH}/Hz	δ terminal BH_3/ppm	J_{BH}/Hz
$Me_3N{-}BH_2{-}NMe_2{-}BH_3$ (**1**)	3.2 (t)	111	−13.0 (q)	92
$Me_3N{-}BH_2{-}NHMe{-}BH_3$ (**2**)	0.1 (t)	108	−17.0 (q)	92
$MeNH_2{-}BH_2{-}NHMe{-}BH_3$ (**3**)	−6.2 (t)	106	−19.3 (q)	92

dx.doi.org/10.1021/ja404247r | J. Am. Chem. Soc. 2013, 135, 12670−12683

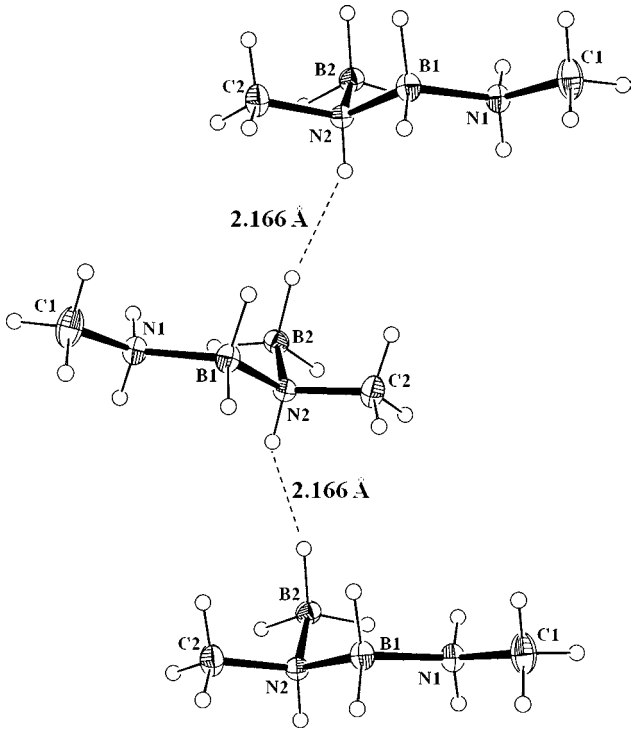

Figure 1. Intermolecular BH−HN interactions between molecules of **3** in the solid state.

actions between adjacent molecules, producing distinct pairs of diborazanes in the solid state.[45]

The B−N bond length between the terminal amine and internal borane moiety (B1−N1) in **2** (see Figure SI-1) was elongated relative to that present in **3**, presumably due to the increased steric bulk of Me_3N relative to $MeNH_2$ (Table 2). A similar elongation is also reported for the related amine-borane adducts $Me_3N{\cdot}BH_3$, B−N = 1.617(6) Å, and $MeNH_2{\cdot}BH_3$, B−N = 1.594(1) Å.[52] The bond between the terminal boron and the internal nitrogen center in **2** was also found to be elongated relative to that in **3**, presumably as a result of a similar effect.

2. Reactivity of Linear Diborazanes. *(a). Reactivity of Me_3N−BH_2−NMe_2−BH_3 (1).* The reactivity of the fully N-methylated diborazane **1** was initially studied by Burg and Randolph, in 1949.[42] Thermolysis of **1** at 80 °C in the absence of solvent was reported to result in its redistribution to form $Me_3N{\cdot}BH_3$ (**8**) and $[Me_2N\text{-}BH_2]_2$ (**9a**), with the latter presumably formed via the dimerization of an initially formed monomeric aminoborane $Me_2N{=}BH_2$ (**9b**). We therefore chose to begin our studies of diborazane reactivity with this compound, initially by verifying the results of Burg. Indeed, on heating a THF solution of this diborazane to 70 °C over 2 h, ^{11}B NMR spectroscopy indicated clean formation of amine-borane **8** (δ_B = −8.8 ppm [q, J_{BH} = 98 Hz])[53] and cyclodiborazane **9a** (δ_B = 4.3 ppm [t, J_{BH} = 112 Hz])[45] (Scheme 7(i)).[54]

Next, we studied the analogous reaction of linear diborazane **1** in the presence of the Ir pincer catalyst IrH_2POCOP,[55] which

Scheme 7. Thermal (i) and Catalytic (ii) Redistribution of Diborazane 1

$$\underset{\mathbf{1}}{Me_3N\text{-}BH_2\text{-}NMe_2\text{-}BH_3} \xrightarrow[\text{(ii) 1 mol \% [Ir]}]{\text{(i) 70 °C, THF}} \underset{\mathbf{8}}{Me_3N{\cdot}BH_3} + \tfrac{1}{2}\underset{\mathbf{9a}}{[Me_2N\text{-}BH_2]_2}$$

has been demonstrated to be an efficient dehydropolymerization catalyst for primary amine-boranes.[12,13,15] A solution of **1** in d_8-THF was, therefore, treated with 1 mol % IrH_2POCOP over 4 h at 20 °C, and the reaction course was monitored by ^{11}B NMR spectroscopy. As with the thermal process, the reaction was found to cleanly yield **8** and **9a** except that in this case these products were formed at room temperature (Scheme 7(ii)). The monomeric aminoborane, **9b**, was also observed in small amounts in the early stages of the reaction as an intermediate by ^{11}B NMR spectroscopy (δ_B = 37.0 ppm [t, J_{BH} = 130 Hz]).[56] This species was presumably an initial product of the redistribution, before cyclodimerization proceeded to form **9a** as a final product.

The potential generality of this metal-catalyzed redistribution was subsequently probed through analogous reactions with a range of other amine-borane dehydrocoupling catalysts. Reactions, however, with a 1 mol % loading of either in situ generated $[Cp_2Ti]$,[19] $[Rh(\mu\text{-Cl})cod]_2$[45] or skeletal Ni,[38] produced negligible redistribution by ^{11}B NMR spectroscopy over 4 h at 20 °C, suggesting IrH_2POCOP to be an unusually active catalyst for this transformation. Subsequent catalytic studies with other diborazanes were therefore limited to this Ir complex.

It is significant at this point to note that the complete methylation at nitrogen in **1** renders this species unique among the studied linear diborazanes. In this case, the scope of reactivity is limited by the fact that notionally only one amine-borane/aminoborane pair can be formed upon redistribution due to the presence of the tertiary amine moiety in the terminal position. Furthermore, the final products, amine-borane **8** and cyclodiborazane **9a**, were shown by independent experiment (see the Supporting Information) to be unreactive toward one another at 20 °C over 5 days. Thus, the only further reactivity following the initial redistribution was the dimerization of the monomeric aminoborane product, **9b**, as discussed previously. We therefore viewed diborazane **1** to be a useful model compound for studies of the initial redistribution chemistry that would also be expected to occur for more complex diborazanes **2** and **3** (vide infra), in which additional reactivity would be anticipated due to the presence of N−H as well as B−H bonds.

(b). Reactivity of Me_3N−BH_2−NHMe−BH_3 (2). The reactivity of Me_3N−BH_2−NHMe−BH_3 (**2**) was subsequently investigated under the same regimes as for **1**. In this case, due to the presence of the internal NHMe moiety, additional reactivity compared to that of **1** would be expected, with the potential formation of the primary aminoborane, $MeNH{=}BH_2$ (**10**), of particular significance.

Thermolysis of **2** over 18 h[57] at 70 °C led to complete redistribution to form a series of new products by ^{11}B NMR spectroscopy: amine-borane **8** (δ_B = −8.5 ppm) [53%],

Table 2. Selected Solid State Metrical Parameters for Diborazanes 2 and 3

Diborazane	B1−N1 (Å)	B1−N2 (Å)	N2−B2 (Å)
Me_3N−BH_2−NHMe−BH_3 (**2**)	1.6164(13)	1.5768(14)	1.6067(14)
$MeNH_2$−BH_2−NHMe−BH_3 (**3**)	1.5870(10)	1.5741(9)	1.5896(9)

dx.doi.org/10.1021/ja404247r | J. Am. Chem. Soc. 2013, 135, 12670−12683

$[MeNH\text{-}BH_2]_x$ (**11**) (δ_B = 1.4 to −6.6 ppm) [16%], amine-borane **6** (δ_B = −18.7 ppm) [16%], and borazine $[MeN\text{-}BH]_3$ (**12**) (δ_B = 32.8 ppm) [15%] (Scheme 8(i)). Following

Scheme 8. Catalytic (i) and Thermal (ii) Redistribution of 2

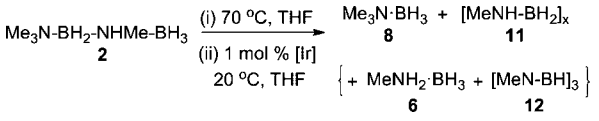

precipitation, **11** was isolated as an oily material. Analysis by electrospray ionization mass spectrometry (ESI-MS) was consistent with an oligomeric structure $[MeNH\text{-}BH_2]_x$ with multiple distributions of repeat unit of m/z 43 ($MeNH{=}BH_2$ = 43.06 Da) observed up to molecular weights of ∼2000 Da (Figures SI-14 and SI-15). No evidence for high molar mass polymeric material (M_n > 5000) could be detected by gel permeation chromatography (GPC), however, which indicated that no significant quantity of high molecular weight poly(methylaminoborane) was formed. It is notable that the ^{11}B NMR signal for the oligomeric species showed more resonances than for high molecular weight polymer (which shows a single broad resonance at ca. −6 ppm),[12,13] and this may be the result of the resolution of different environments (including end groups) near the chain termini or the presence of chain branching, an effect which would be particularly pronounced in relatively short oligomeric species.

Based on the reactivity of diborazane **1** at 70 °C in THF, it was postulated that the likely initial reaction products were the observed amine-borane **8** and transient aminoborane $MeNH{=}BH_2$ (**10**).[58] The latter species presumably spontaneously oligomerizes to produce the cyclic/linear oligomeric final observed products. It has been previously reported that the parent aminoborane, $NH_2{=}BH_2$, which is also a transient species under ambient conditions, can be trapped from solution as the aminodialkylborane $NH_2{=}BCy_2$ by a double hydroboration reaction with cyclohexene.[59−61] We therefore attempted to trap aminoborane **10** in a similar manner, by repeating the thermolysis reaction of diborazane **2** in the presence of 2.5 equiv of cyclohexene. This led again to complete consumption of the diborazane to yield similar products by ^{11}B NMR spectroscopy, but in this case an additional resonance at 45.0 ppm (19% of total ^{11}B content) was also identified and was assigned as $MeNH{=}BCy_2$ (**13**).[62,63]

Under catalytic conditions the products observed from the redistribution of diborazane **2** were, as in the case of **1**, the same as those formed by thermolysis. Thus, upon treatment of a THF solution of **2** with 1 mol % IrH_2POCOP at 20 °C, monitoring by ^{11}B NMR spectroscopy indicated complete consumption of the initial diborazane over 6 h to give a product mixture that contained **8** [51%], **11** [28%], **6** [8%] and **12** [13%] (Scheme 8(ii)). Analysis of the oily solids attained by precipitation of the reaction mixture into hexanes by ESI-MS again confirmed the generation of oligomeric products of the form $[MeNH\text{-}BH_2]_x$ (**11**), with oligomeric distributions of repeat unit of m/z = 43 apparent (Figure 2). Once more, however, analysis by GPC indicated the absence of a high molar mass fraction with M_n > 5000.[64]

As for the analogous thermal process, the presence of aminoborane **10** within the mixture was probed through the addition of cyclohexene to the reaction. In this case, and in contrast to the thermolysis experiment, addition of the olefin

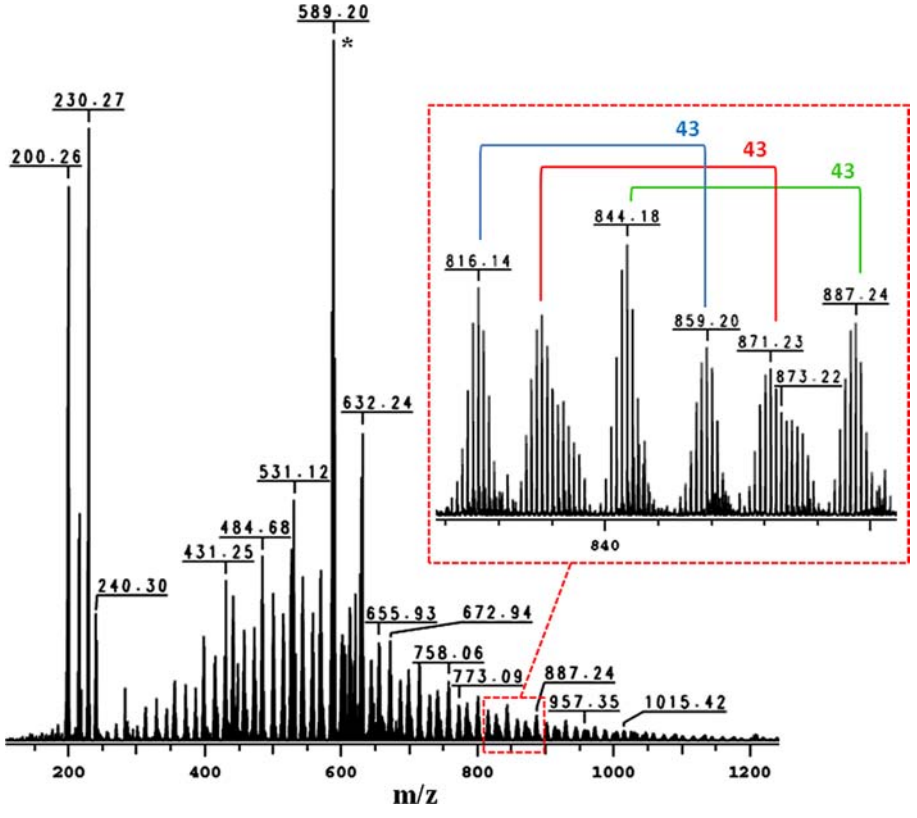

Figure 2. ESI mass spectrum of $[MeNH\text{-}BH_2]_x$ (**11**) produced via reaction of **2** and IrH_2POCOP. ∗ = $IrPOCOP\text{-}H^+$. Inset evidences multiple oligomeric distributions of repeat unit 43 Da.

dx.doi.org/10.1021/ja404247r | J. Am. Chem. Soc. 2013, 135, 12670−12683

did not lead to the formation of detectable quantities of the hydroboration product **13** based on ^{11}B NMR spectroscopy. Instead, the formation of a comparable oligomeric product (**11**) to that observed in the absence of the trapping agent was detected by NMR spectroscopy and ESI mass spectrometry, along with similar quantities of the previously observed **8**, **6**, and **12**. The inability to trap aminoborane **10** despite the formation of **11**, may indicate that **10** remains bound to, or reacts rapidly with, the metal center during both the redistribution and polymerization,[13,36] and hence is not free in solution for sufficiently long to allow reaction with cyclohexene. A similar postulate has been made by Baker and co-workers to explain the lack of trapping of NH_2=BH_2 in the presence of cyclohexene during the dehydrogenation of NH_3·BH_3 using the same Ir catalyst.[59] In addition, the proposed binding of aminoborane within the coordination sphere of the Ir center is made more reasonable by the growing number of well-characterized metal-bound aminoborane species that have been recently reported,[27,65−72] with examples of relevant complexes of the primary aminoborane *t*BuNH=BH_2 reported by Weller, $[((PCy)_3)_2Ir(H)_2(\mu\text{-}H)_2BNHtBu][BAr^f{}_4]$,[70] and by Aldridge, $[(IMes)_2Rh(H)_2(\mu\text{-}H)_2BNHtBu][BAr^f{}_4]$,[72] respectively (see Figure 3).

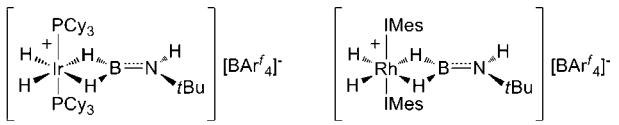

14 **15**

Figure 3. Group 9 metal complexes of *t*BuNH=BH_2, as reported by Weller (**14**)[70] and Aldridge (**15**).[72]

The formation of a small amount of borazine **12** and amine-borane **6** from **2** under both thermolytic and catalytic conditions in this case might be expected to result from H_2 transfer reactions[73] between the initial products, amine-borane **8** and aminoborane **10**, and unreacted diborazane. The reaction of **8** with diborazane **2** was initially explored to probe this postulate, with no reaction apparent at ambient temperature in THF solution by ^{11}B NMR spectroscopy, nor any effect on the product distribution observed upon thermolysis of the mixture. Directly probing the potential hydrogen transfer chemistry of the second reaction product, aminoborane **10**, by similar means was, however, not possible due to the transient nature of this species. As an alternative, we therefore chose to investigate the reactivity of **2** with *i*Pr_2N=BH_2, a sterically encumbered model aminoborane, stable in its monomeric form at ambient temperature.[74] When diborazane **2** was treated with a stoichiometric amount of *i*Pr_2N=BH_2 in THF solution (20 °C, 18 h) ∼55% consumption of **2** to form the previously discussed redistribution products of **2** including **12** and **6**,[75,76] along with the aminoborane hydrogenation product *i*Pr_2NH·BH_3 (20%) was observed by ^{11}B NMR spectroscopy. This clearly demonstrated the likely reactivity of in situ generated aminoboranes such as **10** toward linear diborazanes under the conditions used for the redistribution reactions.

*(c). Reactivity of $MeNH_2$–BH_2–NHMe–BH_3 (**3**).* We next explored the reactivity of symmetrically substituted diborazane **3**, a potential intermediate in the formation of high molecular weight poly(methylaminoborane), $[MeNH\text{-}BH_2]_n$ (**16**) from **6**.[36] Heating a THF solution of diborazane **3** to 70 °C for 18 h[57] resulted in an almost quantitative conversion of **3** to amine-borane **6** (δ_B = −18.9 ppm [q, J_{BH} = 94 Hz])[45] and the cyclic triborazane $[MeNH\text{-}BH_2]_3$ (**17**) (δ_B = −5.2 ppm [t, J_{BH} = 101 Hz]),[77] together with a small amount of borazine **12**[45] by ^{11}B NMR spectroscopy (Scheme 9a). Analysis of the reaction

Scheme 9. (a) Thermolysis of 3 and (b) Thermolysis of 3 with in Situ Cyclohexene Trapping

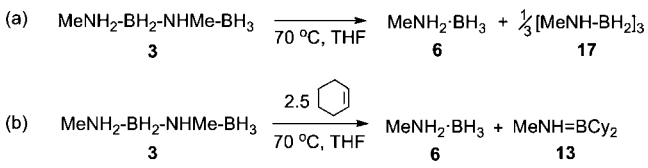

mixture by ESI-MS and GPC was attempted in anticipation of the formation of a minor amount of oligoaminoborane **11** in addition to cyclotriborazane **17**, as was observed with diborazane **2** by ESI-MS. Indeed, ESI-MS confirmed the formation of oligomeric **11**, with at least three different distributions of repeat unit with *m*/*z* 43 observed up to molecular weight of ∼2000 Da (Figures SI-16 and SI-17). No evidence, however, of high molecular weight polymeric material could be detected by GPC, which was consistent with the results for the thermolysis of linear diborazane **2**. Cyclotriborazane **17** was postulated to form from the trimerization of aminoborane **10**, the presence of which was once again probed through cyclohexene trapping. Repeating the thermolysis of **3** for 18 h at 70 °C in the presence of 2.5 equiv of cyclohexene, therefore, yielded both amine-borane **6** and the expected trapping product MeNH=BCy_2 (**13**) in an approximately 1:1 ratio (Scheme 9b). The latter species was in this case isolable as a colorless oil for complete characterization by multinuclear NMR spectroscopy and high resolution mass spectrometry (HR-MS) (see the Supporting Information).

The formation of **13** strongly implicates the generation of *free* aminoborane **10** in the thermal redistribution of diborazane **3**. It was also notable that the thermolysis of **3** in the presence of cyclohexene did not lead to the formation of detectable concentrations of borazine **12**, as was observed in its absence. This suggested that the presence of cyclohexene, and thus trapping of free aminoborane MeNH=BH_2 (**10**), prevents the formation of **12**.

The effect of in situ generated aminoborane **10** in the reaction mixture was subsequently probed with the model aminoborane *i*Pr_2N=BH_2, as for the case of **2**. Reaction of **3** and *i*Pr_2N=BH_2 (18 h, 20 °C) in THF solution led to complete consumption of **3**, hydrogenation of *i*Pr_2N=BH_2 to *i*Pr_2NH·BH_3 (80%), and the formation of a complex mixture of products including amine-borane **6** (30%), amidodiborane **4** (8%), cyclotriborazane **17** (25%), and borazine **12** (9%) by ^{11}B NMR spectroscopy (Scheme 10). Thus, the significant reactivity of aminoboranes with diborazanes was once again demonstrated, with the increased quantity of **12** relative to that observed upon thermolysis of **3** possibly further implicating

Scheme 10. Reaction of 3 and *i*Pr_2N=BH_2 (THF, 20 °C, 18 h)

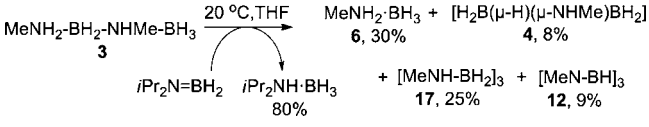

dx.doi.org/10.1021/ja404247r | J. Am. Chem. Soc. 2013, 135, 12670−12683

aminoborane **10** in their formation under thermolytic conditions.

The behavior of diborazane **3** under iridium catalysis was, however, markedly different to that observed under thermolysis. Treatment of a THF solution of **3** with 0.6 mol % IrH_2POCOP[78] at 20 °C over 1.5 h resulted in complete conversion of **3** to a single new species, appearing as a broad singlet in the ^{11}B NMR spectrum at −6 ppm (Scheme 11a),

Scheme 11. Proposed Mechanism of Polymerization of (a) 3 and (b) 6 with 0.3 mol % IrH_2POCOP

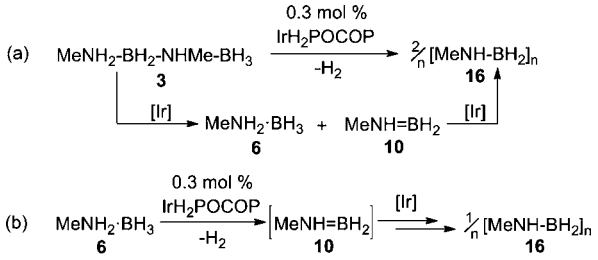

with amine-borane **6** detected as an intermediate (δ_B = −18.7 ppm [q, J_{BH} = 94 Hz]).[79] The product was isolated as an off-white solid via precipitation into hexanes in 86% yield. Analysis by multinuclear NMR spectroscopy confirmed the product to be the polyaminoborane $[MeNH{-}BH_2]_n$, (**16**), which was spectroscopically identical to the same material produced from amine-borane **6** (see the Supporting Information). Analysis of the polymer by GPC indicated a M_w of 97 000 Da, and PDI of 1.44, and ESI-MS analysis was indicative of a material of linear polymeric distribution with a repeat unit of m/z = 43, as observed for the same polymer produced from **6**.[13]

The presence of free aminoborane **10** in the Ir-catalyzed reaction of **3** was investigated, as for the case of **2**, via the addition of cyclohexene as a trapping agent. Once again, and as expected for the postulated on-metal polymerization, cyclohexene addition did not lead to the formation of the trapping product **13** that was observed under thermal conditions. Instead the high molar mass polyaminoborane **16** was once again isolated as the sole product.[80] We therefore postulate that the formation of **16** from **3**, as with the case of **2**, occurs without aminoborane **10** being present as a free species in solution for a significant length of time. Either the polymerization occurs without release of **10** into solution or the reaction of any **10** released into solution with the Ir center is so rapid that cyclohexene trapping is ineffective. (Scheme 11a). A similar tentative mechanistic conclusion in favor of the operation of an "on-metal" process rather than "off-metal" pathway for polyaminoborane formation has previously been made for the Ir-catalyzed dehydropolymerization of **6** to form **16** (Scheme 11b).[13] Further support is provided by the aforementioned metal-mediated diborazane formation at cationic Ir centers (see Scheme 3).[36]

3. Mechanistic Investigations. The experimental studies of the reactivity of linear diborazanes **1** - **3** provided clear evidence for redistribution reactions initiated by thermolysis or an Ir-center to form an amine-borane/aminoborane pair. However, in the cases of **2** and **3**, the complex further reactivity of the initial reaction products limited mechanistic insight into the fundamental redistribution process. However, even in the case of **1** it is possible to postulate at least four potential routes to the redistributed products (Scheme 12).

Scheme 12. Mechanisms Considered for Amine-Borane/Aminoborane Formation from Linear Diborazanes[a]

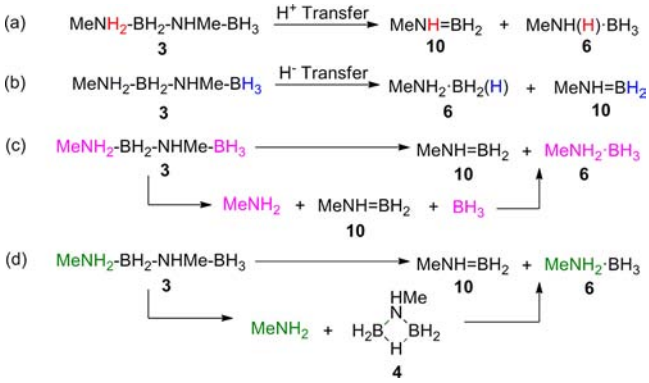

[a]Diborazane **3** is used as an illustrative example.

First, two closely related mechanisms can be proposed, involving proton transfer from N (Scheme 12a) and hydride transfer from B (Scheme 12b) as the respective initial steps. Such transfers may occur intramolecularly or intermolecularly to furnish identical products. It is notable, however, that a proton transfer mechanism cannot operate in linear diborazanes **1** and **2** due to the lack of protic hydrogens at the terminal amine moiety. Second, the diborazane could undergo cleavage of the bonds to the terminal amine and borane moieties, respectively, forming the aminoborane directly, and the amine-borane via combination of the free amine and borane (Scheme 12c). An analogous mechanism has been previously postulated as the mode of redistribution of the related hybrid phosphinoborane/amine-borane chain compounds, $R_2NH{-}BH_2{-}PR_2{-}BH_3$.[81] Finally, as suggested by the case of **1**, it is possible that the reaction of μ-amidodiboranes, $[H_2B(\mu\text{-}H)(\mu\text{-}NR_2)BH_2]$, with free amine, as employed in the synthesis of all of the linear diborazanes **1**−**3**, may be reversible under thermal or catalytic conditions leading to reformation of the free amine and μ-amidodiborane (Scheme 12d). Subsequently, the free amine could then abstract a BH_3 moiety from the μ-amidodiborane under thermal or catalytic conditions to yield the observed amine-borane and aminoborane products.

(a). Mechanism of Thermal Redistribution Reactions. With a view to probing which of the above postulated mechanisms are in operation we attempted to elucidate further mechanistic details using diborazane **1**,[82] for which clean redistribution was observed (Section 2(a)), and stability at ambient temperature over 24 h in THF solution was demonstrated (^{11}B NMR spectroscopy).[83] However, it is notable that, as stated previously, the nature of the substitution in this species precludes the possibility of the proton transfer mechanism in this case (Scheme 12a).

To narrow the scope of mechanistic investigations, it was initially important to ascertain the kinetic order of the redistribution. In preliminary experiments, triplicate thermolyses of **1** (THF, 65 °C,[84] 0.35 M, 14 h) indicated that the reaction was initially first order in linear diborazane (Figure 4), pointing toward a unimolecular redistribution with $k_H = 7.5 \times 10^{-5}$ s^{-1} in the first half-life. To further probe the mechanism of redistribution, the B-deutero diborazane $Me_3N{-}BD_2{-}NMe_2{-}BD_3$ (**1-D**) was prepared from BD_3·THF (see the Supporting Information), and its thermolysis studied, with subsequent analysis of the kinetic isotope effects (KIEs) between the isotopologues allowing elimination of some of the proposed

dx.doi.org/10.1021/ja404247r | J. Am. Chem. Soc. 2013, 135, 12670−12683

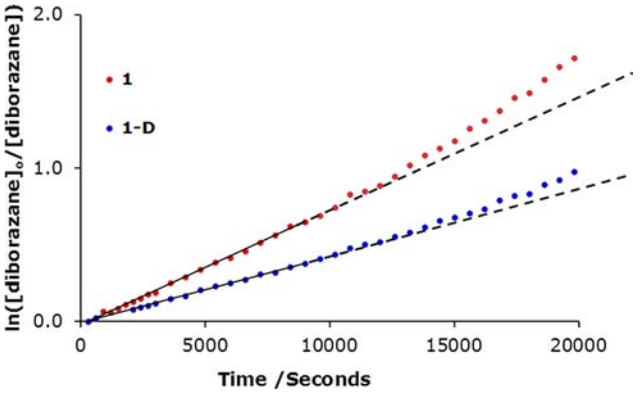

Figure 4. ^{11}B NMR monitoring of the redistribution of diborazane **1** and **1-D** (THF, 65 °C, 0.35 M, 14 h). All points based on average conversions by ^{11}B NMR spectroscopy over three identical runs. Red points = **1**, $k_H = 7.5 \times 10^{-5}$ s^{-1} determined from the slope of linear fit (black line); blue points = **1-D**, $k_D = 4.3 \times 10^{-5}$ s^{-1}. Note the dashed black line is the extrapolated initial linear fit and demonstrates the degree of acceleration at increased conversions.

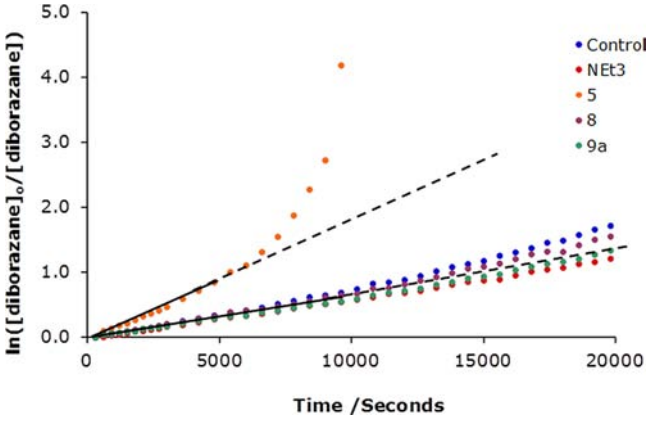

Figure 5. ^{11}B NMR monitoring of the thermal redistribution of 0.35 M **1** averaged over three identical trials (blue), 0.40 M **1** + 0.14 M **5** (orange), 0.35 M **1** + 0.090 M **9a** (green), 0.35 M **1** + 0.19 M **8** (maroon), and 0.35 M **1** + 0.17 M NEt_3 (red) in THF at 65 °C. Note the dashed black line is the extrapolated initial linear fit and demonstrates the degree of deviation from linearity at increased conversions for the control (blue), and with the addition of **5** (orange).

mechanisms. The kinetics of redistribution of **1-D** at 65 °C proceeded more slowly than for **1** ($k_D = 4.3 \times 10^{-5}$ s^{-1}, Figure 4), corresponding to a KIE of 1.7. As a large and normal (primary) KIE between 2 and 10 would be anticipated for *mechanism b* (Scheme 12) due to the cleavage of a B-(H/D) bond in the rate determining step, *mechanism b* can be discounted. *Mechanisms c and d* (Scheme 12), are however, consistent with the measured KIE, which, due to its relatively low magnitude, may arise from a secondary KIE, or from an equilibrium isotope effect.

The first order treatment of the data provided in Figure 4 demonstrated slight deviation from linearity toward increased conversions, which led us to consider the presence of an autocatalyst. In order to determine the source of curvature in the data, the effect of the addition of known quantities of various conceivable intermediates and products (**9a**, **8**, **5**, NEt_3,[85] BH_3·THF) upon the rate of the redistribution reaction was assessed. Most notably, addition of BH_3·THF (0.090 M) to a solution of **1** (0.3 M) resulted in an extremely rapid reaction at *ambient temperature* to form amidodiborane **5** and amine-borane **8**. At 65 °C, the BH_3·THF is very short-lived during the redistribution reactions, with the characteristic peak at $\delta = -1.1$ ppm not observed by ^{11}B NMR spectroscopy as the reaction was monitored. Among the reactions to which **9a**, **8**, **5**, or NEt_3, respectively, were added, only the addition of amidodiborane **5** produced a significant deviation from the kinetics of the control reactions, with this compound significantly accelerating the redistribution reaction (Figure 5). This species, therefore, presented a possible source of the substantial deviation from linearity in the kinetics of redistribution of **1** at increased conversions.

Kinetic simulations of the experimental data from the redistribution of pure **1** and comparison to reactions with added **5** (Figures 6, SI-4, and SI-5) suggested a model that was in fact more complex than a simple autocatalysis reaction of intermediate **5** with **1**, and corroborated the observation that BH_3·THF plays a significant role as it is eliminated from **5** (along with **9b**). The operating mechanism (Scheme 13) is postulated to involve first order redistribution of **1** to yield **5** and NMe_3 (the reverse of the synthetic route to **1**, see Scheme 6) which then undergoes further reaction to form **8** and **9b**. This reaction is in competition with production of **8** via direct reaction of BH_3 with NMe_3, as BH_3·THF is produced from an equilibrium dissociation reaction of μ-amidodiborane **5**, which also yields **9b**. The monomeric aminoborane **9b** is therefore produced in two different ways: through reaction of **5** and NMe_3 and also through dissociation of **5**. Subsequent dimerization then occurs to give **9a**, unless it is rapidly coupled with BH_3 to produce **5** as shown in the k_3/k_{-3} equilibrium.

The small equilibrium constant K_3 ($(8 \pm 4) \times 10^{-7}$ M; $k_{-3} = (3 \pm 2) \times 10^2$ M^{-1}·s^{-1}) coupled with the large value for k_4 ($(10 \pm 5) \times 10^4$ M^{-1}·s^{-1}) would be expected to result in undetectable amounts of BH_3 present in solution, as observed experimentally. The overall redistribution of **1** is driven by reactions k_2 and k_4 which irreversibly produce **8**. This feature of the mechanism is consistent with the observation that the concentration of **8** was measurably larger (ca. 1%) than that of **9a** at early reaction times as a large portion of **9b** was sequestered as **5** and therefore unavailable to dimerize. The redistribution of **1** is limited by its dissociation into **5** and NMe_3 (k_1) and subsequent dissociation of **5** into BH_3 and **9b** (k_3).

At this stage, we also studied the system using DFT calculations[86] to gain further insight into the redistribution pathways and support our postulate that a slightly more complex version of *mechanism d* (Scheme 12) was in operation.[87] Initially, however, we also considered an alternative permutation of *mechanism c* involving a concerted process which invokes a 4-membered cyclic transition state (**1′**) (Scheme 14). On calculating the approach to synperiplanar transition state **1′** required for this pathway a large increase in energy was observed, leading to an insurmountable barrier to redistribution to form the observed amine-borane/amino-borane pair (see the Supporting Information, section (iii) and Figure SI-3). It is particularly illustrative that the least endergonic process, based on the computations, was elimination of Me from the terminal NMe_3 group, a process which, unsurprisingly, was not observed experimentally.[88] This mechanistic pathway was, therefore, also discounted.

Computational investigation of *mechanism d* (B97D/6-31G(d,p)) revealed that the initial dissociation of Me_3N from

dx.doi.org/10.1021/ja404247r | J. Am. Chem. Soc. 2013, 135, 12670−12683

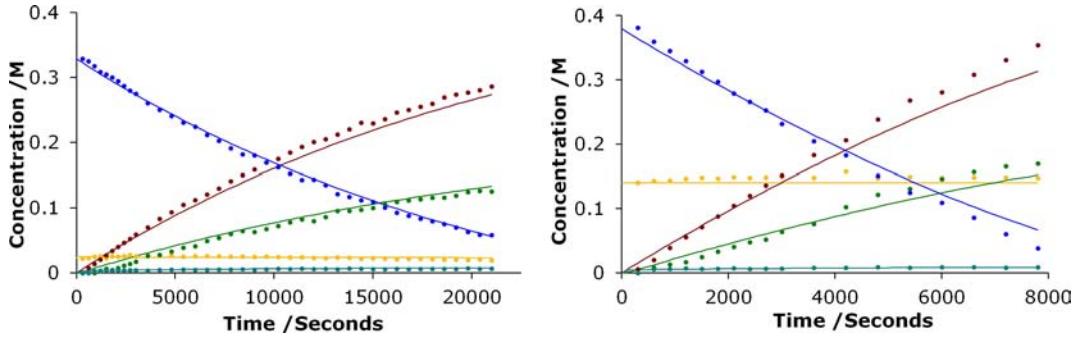

Figure 6. Representative plots from ^{11}B NMR monitoring of the thermal redistribution of 0.35 M **1** (left) and 0.40 M **1** + 0.14 M **5** (right) in THF at 65 °C. The circles represent experimental data, and the solid lines represent simulated data based on the model presented in Scheme 13 (including color-scheme). Data was averaged over four trials (2 × solution of solely **1** and 2 × solution of **1** with 0.14 M **5**).

Scheme 13. Kinetic Model of the Redistribution of 1 in THF at 65 °C Based on Simulations of the Experimental Data[a]

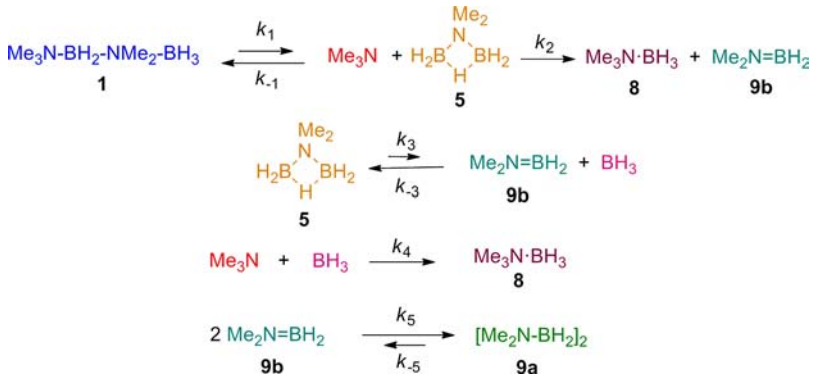

[a]Rates (k) and equilibrium constants (K): $k_1 = 0.09 \pm 0.05$ s^{-1}, $K_1 = (1.2 \pm 0.6) \times 10^4$ M, $k_2 = 0.3 \pm 0.2$ M^{-1}·s^{-1}, $k_3 = (2.7 \pm 0.3) \times 10^{-4}$ M^{-1}·s^{-1}, $K_3 = (8 \pm 4) \times 10^{-7}$ M^{-1}·s^{-1}, $k_4 = (10 \pm 5) \times 10^4$ M^{-1}·s^{-1}, $k_5 = 1.1 \pm 0.2$ M^{-1}·s^{-1}, $K_5 = (2.4 \pm 0.2) \times 10^4$ M^{-1}, see the Supporting Information for further details.

Scheme 14. Unfavorable Concerted Permutation of the Redistribution of Diborazane 1 via *Mechanism c*

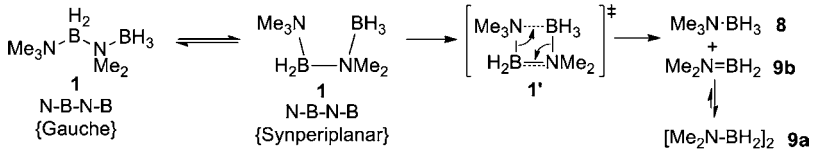

1 to form Me_3N and $[H_2B(\mu\text{-}H)(\mu\text{-}NMe_2)BH_2]$ (**5**) may proceed via two possible transition states, ***gauche*-TS1** and ***anti*-TS1** (Scheme 15(i)) located at 89.4 and 53.8 kJ·mol^{-1}, respectively, above the free energy of the gauche conformer of **1** in THF at 65 °C. Therefore, the reaction, which was predicted to be exergonic by 5.2 kJ·mol^{-1} at that temperature, would be expected to proceed through the lower lying transition state ***anti*-TS1**. Three conceivable routes from Me_3N and **5** to the final products, $Me_2N{=}BH_2$ (**9b**) and $Me_3N{\cdot}BH_3$ (**8**), were then investigated (Scheme 15(ii)). The first possibility involved direct abstraction of BH_3 from amidodiborane **5** by Me_3N via **TS2**,[89] with **TS2** found at 99.1 kJ·mol^{-1}, to form **8** and **9b**. Second, the reaction could occur via a spontaneous elimination of BH_3 from **5** to form a mixture containing Me_3N, BH_3 and **9b**. This step was predicted to be endergonic by 67.2 kJ·mol^{-1}. The associated transition state, **TS3**, could not be located, even in a constrained search (see the Supporting Information, Figure SI-2), suggesting a barrierless process. Subsequent immediate reaction of Me_3N and BH_3 could be expected to rapidly lead to the final products via an exergonic process ($\Delta_R G^\circ_{(338)} = -100.6$ kJ·mol^{-1}). The BH_3 formed by such a process could also be intercepted by THF, present as the solvent, in a further favorable process ($\Delta_R G^\circ_{(338)} = -39.2$ kJ·mol^{-1}), prior to reaction with Me_3N to furnish amine-borane **8** as the final product. Finally, a closely related mechanism was investigated wherein BH_3 is abstracted from **5** by a molecule of THF, via **TS4** ($\Delta G^{\ddagger}_{(338)} = 116.5$ kJ·mol^{-1}), leading to Me_3N, BH_3·THF, and **9b** as discussed previously.

Of the three possible permutations investigated, those occurring via **TS2** and **TS3** are most probable due to their reduced activation energies relative to **TS4**. As previously stated, BH_3·THF was not observed by ^{11}B NMR spectroscopy during experimental studies of this reaction, perhaps favoring, therefore, the reaction via **TS2**. It is likely, however, that reaction of BH_3·THF with Me_3N would be almost instantaneous, particularly at 65 °C, which would prevent significant concentrations of this species building up. This means that the reaction via barrierless spontaneous elimination of BH_3 from **5** (**TS3**) cannot be completely discounted. It can be inferred from the previously observed first order kinetics for the redistribution based on **1** that the initial dissociation of Me_3N

dx.doi.org/10.1021/ja404247r | J. Am. Chem. Soc. 2013, 135, 12670−12683

Scheme 15. Computationally Investigated Permutations of *Mechanism d*[a]

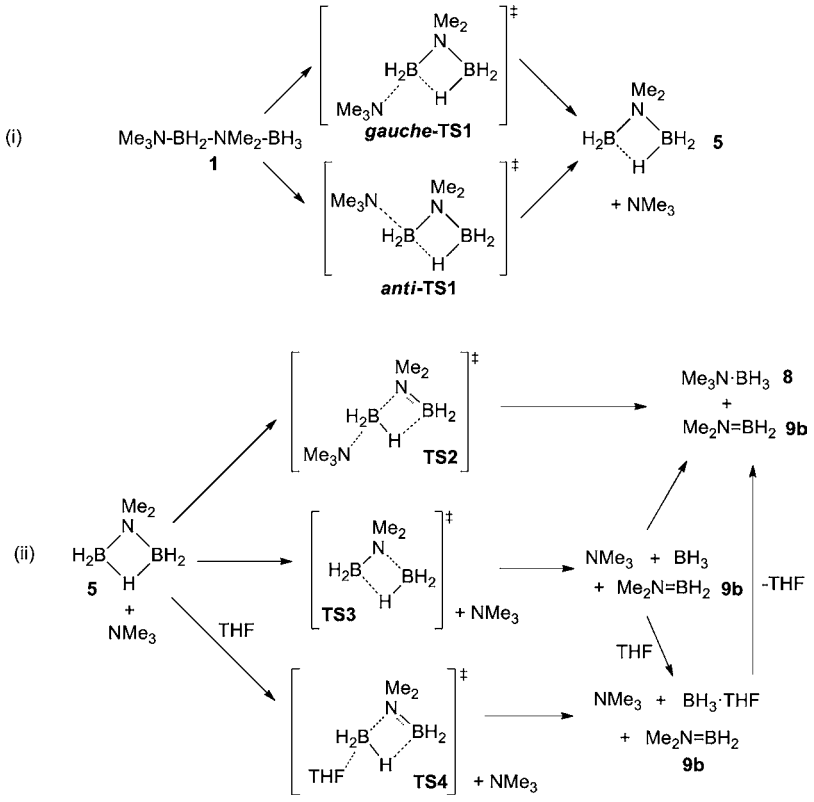

[a](i) Initial dissociation of Me_3N and (ii) further reactions of Me_3N and **5** to yield the final products **9b** and **8**.

via ***anti*-TS1** represents the rate-determining step for the process. Additionally, both routes are also in line with the experimentally calculated KIE for the redistribution, which would be expected to be of low magnitude as no bonds to the labeled atoms are broken during the redistribution.

(b). Mechanism of Metal-Catalyzed Redistributions. To explore the metal-catalyzed redistribution of **1** in more detail the reaction of this species with 2 mol % IrH_2POCOP (0.35 M **1**, 20 °C, THF, 14 h) was monitored by ^{11}B NMR spectroscopy. Again, the data initially fits a pseudo first order dependence on linear diborazane ($k_H = 7.4 \times 10^{-4}$ s^{-1}), with a small amount of deceleration at higher conversions to **8** and **9a** (Figure 7). The effect of deuterium-substitution at boron was also assessed by monitoring redistributions of **1-D**, and yielded $k_D = 8.6 \times 10^{-4}$ s^{-1}. As with the thermolysis of **1**, the absence of a substantial, normal KIE ($k_H/k_D = 0.86$) suggests that there is no B-D bond breaking or making in the rate-determining step of the redistribution, but potentially the presence of an equilibrium isotope effect or a secondary KIE. Through variation of the catalyst loading, the reaction was also found to be first order in [Ir], as evidenced by the observed linear correlation between the rate and [Ir] (Figure 8).

As with the thermolysis experiments, in order to determine the source of curvature in the data at increased conversions during the catalytic redistribution of **1** a series of reactions were performed (20 °C, THF, 1 mol % IrH_2POCOP) with conceivable reactive species added at the start of the monitoring process: 0.23 M **1** + 0.21 M **8**, 0.20 M **1** + 0.12 M **9a**, and 0.20 M **1** + 0.085 M **5** (Figure 9). The monitoring of the catalytic redistribution in the presence of the various additional compounds suggested that the source of curvature in this instance is likely to result from the presence of $Me_3N{\cdot}BH_3$ (**8**)

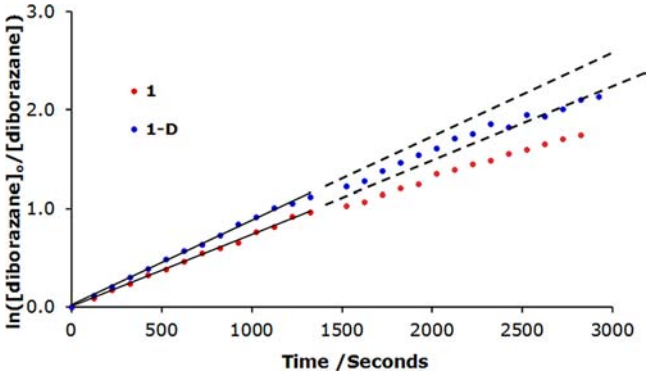

Figure 7. ^{11}B NMR monitoring of the redistribution of diborazane **1** and **1-D** in the presence of IrH_2POCOP (2 mol %, 0.35 M **1**, 20 °C, THF). All points based on average conversions by ^{11}B NMR spectroscopy over two identical runs. Red points = **1**, $k_H = 7.4 \times 10^{-4}$ s^{-1} determined from the slope of linear fit (black line); blue points = **1-D**, $k_D = 8.6 \times 10^{-4}$ s^{-1}. Note the dashed black line is the extrapolated initial linear fit and demonstrates the degree of deceleration at increased conversions.

and $[H_2B(\mu\text{-}H)(\mu\text{-}NMe_2)BH_2]$ (**5**) within the reaction mixture, with these species shown to inhibit the rate of the reaction, in the latter case particularly significantly.

The obvious choice for a model in this case would, therefore, be a mechanism where **5** is produced as an intermediate that subsequently reacts with the Ir-complex rendering it less active (e.g., forming an Ir-adduct in equilibrium with a more active Ir-complex). However, upon simulation of the kinetic data (Figures 10 and SI-6–SI-11), production of **5**, along with NMe_3 as in the thermolytic redistribution of **1**, is not a favored

dx.doi.org/10.1021/ja404247r | J. Am. Chem. Soc. 2013, 135, 12670–12683

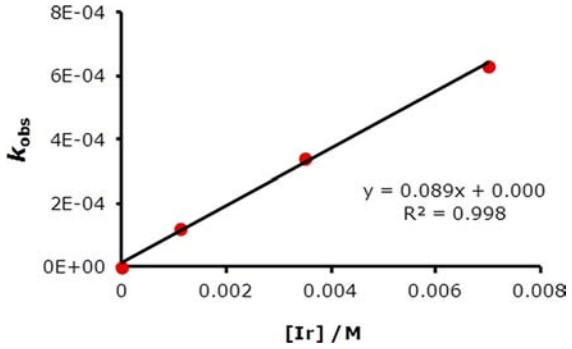

Figure 8. Correlation between rate and Ir-catalyst concentration in the reaction of diborazane **1** and IrH_2POCOP.

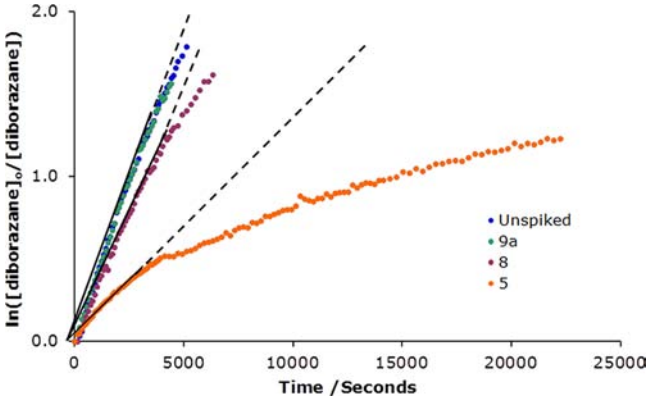

Figure 9. ^{11}B NMR monitoring of the catalytic redistribution of 0.30 M **1** (blue), 0.20 M **1** + 0.09 M **5** (orange), 0.20 M **1** + 0.12 M **9a** (green), and 0.23 M **1** + 0.21 M **8** (maroon), in THF at 20 °C with 1 mol % IrH_2POCOP. Note the dashed black line is the extrapolated initial linear fit and demonstrates the degree of deviation from linearity at increased conversions for reaction of pure **1** (blue), **1** with added **8** (maroon), and **1** with added **5** (orange).

pathway (see the Supporting Information). The model instead suggests that **1** redistributes directly to products **8** (via [Ir]-$H_3B{\cdot}NMe_3$, **Int8**, Scheme 16) and **9b** assisted by an Ir-containing intermediate, $[Ir]{-}H_3B{-}NMe_2{-}BH_2{-}NMe_3$ (**Int1**, Scheme 16). Moreover, the deviation from pseudo first order kinetics (i.e., the curvature apparent in Figure 9) arises from equilibration between **Int8** and **Int1**. At early reaction times when the concentration of **1** is high, **Int1** predominates, which is productive in redistributing to **9b** and **Int8**. As the reaction progresses and produces **8** in appreciable amounts, more of the Ir is present as **Int8**, which progressively inhibits the catalytic turnover. Significantly, both **Int1** and **Int8** are feasible intermediates for which literature precedent exists.[36,37,65,72,90] Furthermore, the reaction of IrH_2POCOP with $Me_3N{\cdot}BD_3$ (**8-D**) demonstrated scrambling of deuterium onto the Ir-center through the disappearance of the Ir−H peaks in the ^1H NMR spectrum ($\delta_H = -17.0$ ppm (t, $J_{HP} = 8$ Hz)) indicating that the "BD_3" moiety in **8-D** interacts with the Ir-center (^2H NMR spectroscopy: $\delta_D = -17.1$ ppm (br s)).

A further remarkable feature of this system elucidated by kinetic modeling was the fact that the dimerization of **9b** to yield **9a**, in addition to occurring spontaneously in an off-metal fashion, appears to be catalyzed by **Int8** (k_3)[27] (k_4, k_{-4}, negligible relative to the other two in this case). This reaction is driven by the irreversible reaction k_2 producing **9b** and is limited by the formation of **Int1** from **Int8** (k_{-1}) to allow for this productive process (k_2) to occur.

CONCLUSIONS

The reactivity of three related diborazanes, $Me_3N{-}BH_2{-}NMe_2{-}BH_3$ (**1**), $Me_3N{-}BH_2{-}NHMe{-}BH_3$ (**2**), and $MeNH_2{-}BH_2{-}NHMe{-}BH_3$ (**3**), under thermal and catalytic conditions has been explored in detail, with the mechanism of their redistribution to form amine-borane/aminoborane pairs elucidated by experimental means, kinetic modeling, and DFT calculations.

Thermolysis of the fully N-methylated diborazane **1** revealed a redistributive process which forms the amine-borane $Me_3N{\cdot}BH_3$ (**8**) and cyclodiborazane $[Me_2N{-}BH_2]_2$ (**9a**) as the sole reaction products. Identical products were also observed under ambient conditions in the presence of catalytic amounts of IrH_2POCOP. The two further diborazanes, **2** and **3**, exhibited similar redistributive chemistry as an initial step, again leading to an amine-borane/aminoborane pair as the initial redistribution products. However, in these cases the formation of $MeNH{=}BH_2$ (**10**) led to complex further reactivity and the formation of oligo- or polyaminoboranes **11** and **16** under both thermal and catalytic conditions. Evidence for the presence of free **10** in solution during the thermolysis reactions was provided by trapping reactions with cyclohexene, in direct contrast to the corresponding metal-mediated reactions in which no analogous trapping was apparent. This suggested that in the presence of the Ir catalyst oligomerization either occurs solely in an "on-metal" process or that any free **10** generated in solution has a very short lifetime and reacts much more rapidly at the metal center than with the cyclohexene trap.

Analysis of the kinetics of the thermal redistribution of diborazane **1**, which was selected as a model system, suggested

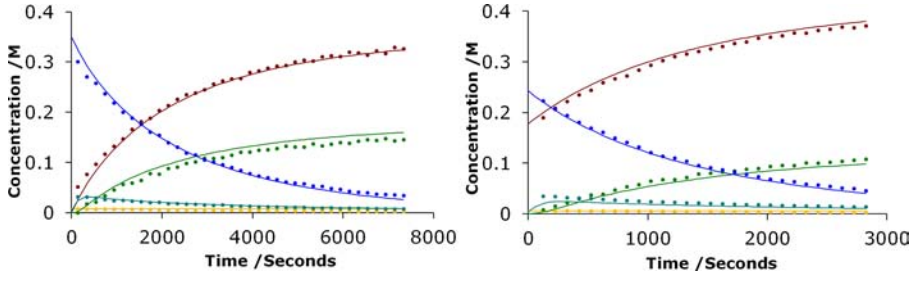

Figure 10. Representative plots from ^{11}B NMR monitoring of the catalytic redistribution of 0.35 M **1** (left) and 0.23 M **1** + 0.21 M **8** (right) in THF at 20 °C with 1 mol % IrH_2POCOP. The circles represent experimental data and the solid lines represent simulated data based on the model presented in Scheme 16 (including color-scheme). Data was averaged over eight trials (2 × 0.3 mol % Ir, 2 × 1 mol % Ir, 2 × 2 mol % Ir, 2 × 1 mol % Ir with added 0.21 M **8**). The orange circles and solid line correspond to species **5**.

dx.doi.org/10.1021/ja404247r | J. Am. Chem. Soc. 2013, 135, 12670−12683

Scheme 16. Simplified Kinetic Model of Redistribution of 1 in the Presence of IrH_2POCOP ([Ir])[a]

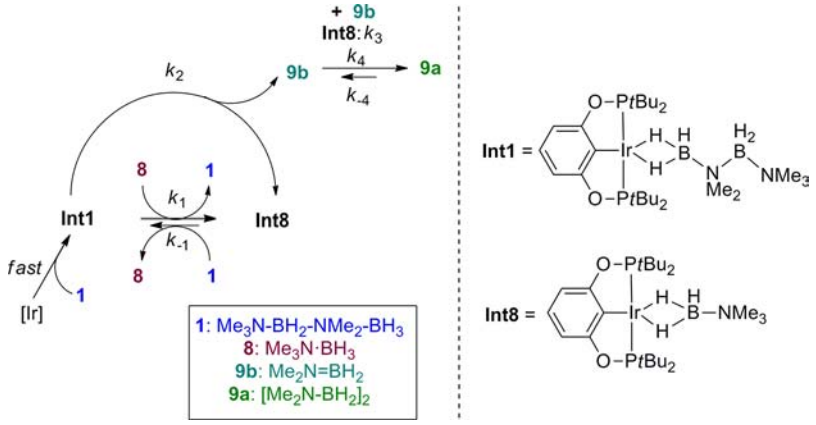

[a]Rate and equilibrium constants from reactions in THF at 20 °C: $k_1 = 6.4 \pm 0.3\ M^{-1}\cdot s^{-1}$, $K_1 = (4 \pm 1) \times 10^1$, $k_2 = 2.5 \pm 0.2\ s^{-1}$, $k_3 = 15 \pm 3\ M^{-1}\cdot s^{-1}$, $k_4 = 2.3 \times 10^{-2}\ M^{-1}\cdot s^{-1}$, $K_4 = 1.0 \times 10^5\ M^{-1}$.

that this reaction initially occurred via a unimolecular process. Based on DFT studies this is likely to involve dissociation of Me_3N from **1**, followed by loss and capture, or abstraction, of BH_3 by Me_3N to yield the amine-borane **8** and also the aminoborane $Me_2N{=}BH_2$ (**9b**), which subsequently dimerizes to form cyclodiborazane **9a**. Deuterium labeling studies of **1** yielded a KIE of 1.7, in line with the proposed mechanism. Modeling of the kinetic data suggested that an observed deviation from simple first-order kinetics within the redistribution of **1** can be attributed to an autocatalytic effect of μ-amidodiborane **5**, formed as an intermediate following the initial dissociation of Me_3N.

In contrast, the mechanism of the Ir-catalyzed redistribution of **1** was found to proceed via a more direct route to yield **9a** and **8** where intermediates **5** and Me_3N were not formed, and the key intermediates are Ir-bound forms of diborazane **1** and amine-borane **8**, respectively. The progressive deviation from first order kinetics, in this case a deceleration in rate, was attributed through kinetic modeling to catalyst inhibition by coordination of **8**, a primary reaction product. It is conceivable that a similar inhibition of the Ir catalyst may hamper the formation of high molecular weight polyaminoborane in the metal-catalyzed redistribution of **2** in which **8** is also formed, as high molar mass **16** was isolated in the corresponding reaction with **3**.

In summary, we have shown that although analogous products are formed, the mechanisms of the thermal and catalytic redistributions of linear diborazanes differ significantly. These results should facilitate further understanding of the complex mechanisms of dehydrocoupling/dehydrogenation reactions of amine-boranes. In addition, they provide support for the proposal that a metal center is required for the formation of high molar mass polyaminoboranes, although in the presence of an inhibitor, or the absence of a metal catalyst altogether, the formation of oligomeric material is preferred.

■ ASSOCIATED CONTENT

Supporting Information

Details of all experiments along with crystallographic information. Full details of additional experiments are also described. This material is available free of charge via the Internet at http://pubs.acs.org.

■ AUTHOR INFORMATION

Corresponding Author

holger.helten@ac.rwth-aachen.de; guy.lloyd-jones@bris.ac.uk; Ian.Manners@bris.ac.uk

Notes

The authors declare no competing financial interest.

■ ACKNOWLEDGMENTS

A.P.M.R, E.M.L., and I.M. acknowledge the EPSRC for funding. T.J. and E.M.L. acknowledge the EU for Marie Curie postdoctoral fellowships. H.H. acknowledges the Deutsche Forschungsgemeinschaft (DFG) for funding within the Emmy Noether Programme. G.C.L.-J. is a Wolfson Research Merit Award Holder. The authors wish to thank Dr. Paul J. Gates of the University of Bristol Mass Spectrometry Facility for useful discussions.

■ REFERENCES

(1) Hutchins, R. O.; Learn, K.; Nazer, B.; Pytlewski, D.; Pelter, A. *Org. Prep. Proced. Int.* **1984**, *16*, 335−372.
(2) Staubitz, A.; Robertson, A. P. M.; Sloan, M. E.; Manners, I. *Chem. Rev.* **2010**, *110*, 4023−4078.
(3) Sanyal, U.; Jagirdar, B. R. *Inorg. Chem.* **2012**, *51*, 13023−13033.
(4) Sloan, M. E.; Staubitz, A.; Lee, K.; Manners, I. *Eur. J. Org. Chem.* **2011**, 672−675.
(5) Yang, X.; Fox, T.; Berke, H. *Chem. Commun.* **2011**, *47*, 2053−2055.
(6) Yang, X.; Fox, T.; Berke, H. *Org. Biomol. Chem.* **2012**, *10*, 852−860.
(7) Stephens, F. H.; Pons, V.; Baker, R. T. *Dalton Trans.* **2007**, 2613−2626.
(8) Jiang, Y.; Blacque, O.; Fox, T.; Frech, C. M.; Berke, H. *Organometallics* **2009**, *28*, 5493−5504.
(9) Yang, X.; Zhao, L.; Fox, T.; Wang, Z.-X.; Berke, H. *Angew. Chem., Int. Ed.* **2010**, *49*, 2058−2062.
(10) Smythe, N. C.; Gordon, J. C. *Eur. J. Inorg. Chem.* **2010**, 509−521.
(11) Sutton, A. D.; Burrell, A. K.; Dixon, D. A.; Garner, E. B.; Gordon, J. C.; Nakagawa, T.; Ott, K. C.; Robinson, J. P.; Vasiliu, M. *Science* **2011**, *331*, 1426−1429.
(12) Staubitz, A.; Presa Soto, A.; Manners, I. *Angew. Chem., Int. Ed.* **2008**, *47*, 6212−6215.
(13) Staubitz, A.; Sloan, M. E.; Robertson, A. P. M.; Friedrich, A.; Schneider, S.; Gates, P. J.; Schmedt auf der Günne, J.; Manners, I. *J. Am. Chem. Soc.* **2010**, *132*, 13332−13345.

(14) Ewing, W. C.; Marchione, A.; Himmelberger, D. W.; Carroll, P. J.; Sneddon, L. G. *J. Am. Chem. Soc.* **2011**, *133*, 17093−17099.
(15) Dietrich, B. L.; Goldberg, K. I.; Heinekey, D. M.; Autrey, T.; Linehan, J. C. *Inorg. Chem.* **2008**, *47*, 8583−8585.
(16) Liu, Z.; Song, L.; Zhao, S.; Huang, J.; Ma, L.; Zhang, J.; Lou, J.; Ajayan, P. M. *Nano Lett.* **2011**, *11*, 2032−2037.
(17) Whittell, G. R.; Manners, I. *Angew. Chem., Int. Ed.* **2011**, *50*, 10288−10289.
(18) Paul, A.; Musgrave, C. B. *Angew. Chem., Int. Ed.* **2007**, *46*, 8153−8156.
(19) Sloan, M. E.; Staubitz, A.; Clark, T. J.; Russell, C. A.; Lloyd-Jones, G. C.; Manners, I. *J. Am. Chem. Soc.* **2010**, *132*, 3831−3841.
(20) Luo, Y.; Ohno, K. *Organometallics* **2007**, *26*, 3597−3600.
(21) Friedrich, A.; Drees, M.; Schneider, S. *Chem.—Eur. J.* **2009**, *15*, 10339−10342.
(22) Blaquiere, N.; Diallo-Garcia, S.; Gorelsky, S. I.; Black, D. A.; Fagnou, K. *J. Am. Chem. Soc.* **2008**, *130*, 14034−14035.
(23) Yang, X.; Hall, M. B. *J. Am. Chem. Soc.* **2008**, *130*, 1798−1799.
(24) Zimmerman, P. M.; Paul, A.; Zhang, Z.; Musgrave, C. B. *Angew. Chem., Int. Ed.* **2009**, *48*, 2201−2205.
(25) Zimmerman, P. M.; Paul, A.; Zhang, Z.; Musgrave, C. B. *Inorg. Chem.* **2009**, *48*, 1069−1081.
(26) Sewell, L. J.; Lloyd-Jones, G. C.; Weller, A. S. *J. Am. Chem. Soc.* **2012**, *134*, 3598−3610.
(27) Stevens, C. J.; Dallanegra, R.; Chaplin, A. B.; Weller, A. S.; MacGregor, S. A.; Ward, B.; McKay, D.; Alcaraz, G.; Sabo-Etienne, S. *Chem.—Eur. J.* **2011**, *17*, 3011−3020.
(28) Vogt, M.; de Bruin, B.; Berke, H.; Trincado, M.; Grützmacher, H. *Chem. Sci.* **2011**, *2*, 723−727.
(29) Ryschkewitsch, G. E.; Wiggins, J. W. *Inorg. Chem.* **1970**, *9*, 314−317.
(30) Beachley, O. T., Jr. *Inorg. Chem.* **1967**, *6*, 870−874.
(31) Helten, H.; Dutta, B.; Vance, J. R.; Sloan, M. E.; Haddow, M. F.; Sproules, S.; Collison, D.; Whittell, G. R.; Lloyd-Jones, G. C.; Manners, I. *Angew. Chem., Int. Ed.* **2013**, *52*, 437−440.
(32) Stephens, F. H.; Baker, R. T.; Matus, M. H.; Grant, D. J.; Dixon, D. A. *Angew. Chem., Int. Ed.* **2007**, *46*, 746−749.
(33) Beweries, T.; Thomas, J.; Klahn, M.; Schulz, A.; Heller, D.; Rosenthal, U. *ChemCatChem* **2011**, *3*, 1865−1868.
(34) Rossin, A.; Bottari, G.; Lozano-Vila, A. M.; Paneque, M.; Peruzzini, M.; Rossi, A.; Zanobini, F. *Dalton Trans.* **2013**, *42*, 3533−3541.
(35) Malcolm, A. C.; Sabourin, K. J.; McDonald, R.; Ferguson, M. J.; Rivard, E. *Inorg. Chem.* **2012**, *51*, 12905−12916.
(36) Johnson, H. C.; Robertson, A. P. M.; Chaplin, A. B.; Sewell, L. J.; Thompson, A. L.; Haddow, M. F.; Manners, I.; Weller, A. S. *J. Am. Chem. Soc.* **2011**, *133*, 11076−11079.
(37) Dallanegra, R.; Chaplin, A. B.; Tsim, J.; Weller, A. S. *Chem. Commun.* **2010**, *46*, 3092−3094.
(38) Robertson, A. P. M.; Suter, R.; Chabanne, L.; Whittell, G. R.; Manners, I. *Inorg. Chem.* **2011**, *50*, 12680−12691.
(39) Spielmann, J.; Jansen, G.; Bandmann, H.; Harder, S. *Angew. Chem., Int. Ed.* **2008**, *47*, 6290−6295.
(40) Liptrot, D. J.; Hill, M. S.; Mahon, M. F.; MacDougall, D. J. *Chem.—Eur. J.* **2010**, *16*, 8508−8515.
(41) Hill, M. S.; Kociok-Köhn, G.; Robinson, T. P. *Chem. Commun.* **2010**, *46*, 7587−7589.
(42) Burg, A. B.; Randolph, C. L., Jr. *J. Am. Chem. Soc.* **1949**, *71*, 3451−3455.
(43) Robertson, A. P. M.; Leitao, E. M.; Manners, I. *J. Am. Chem. Soc.* **2011**, *133*, 19322−19325.
(44) Nöth, H.; Thomas, S. *Eur. J. Inorg. Chem.* **1999**, 1373−1379.
(45) Jaska, C. A.; Temple, K.; Lough, A. J.; Manners, I. *J. Am. Chem. Soc.* **2003**, *125*, 9424−9434.
(46) Chen, X.; Zhao, J.-C.; Shore, S. G. *J. Am. Chem. Soc.* **2010**, *132*, 10658−10659.
(47) Hahn, G. A.; Schaeffer, R. *J. Am. Chem. Soc.* **1964**, *86*, 1503−1504.
(48) Schlesinger, H. I.; Ritter, D. M.; Burg, A. B. *J. Am. Chem. Soc.* **1938**, *60*, 2297−2300.
(49) For an example of the analogous reactivity with N-heterocyclic carbenes, see Sabourin, K. J.; Malcolm, A. C.; McDonald, R.; Ferguson, M. J.; Rivard, E. *Dalton Trans.* **2013**, *42*, 4625−4632.
(50) We have previously briefly reported the synthesis and structure of diborazane **3** in a communication: see ref 36.
(51) Jaska, C. A.; Manners, I. *J. Am. Chem. Soc.* **2004**, *126*, 9776−9785.
(52) Aldridge, S.; Downs, A. J.; Tang, C. Y.; Parsons, S.; Clarke, M. C.; Johnstone, R. D. L.; Robertson, H. E.; Rankin, D. W. H.; Wann, D. A. *J. Am. Chem. Soc.* **2009**, *131*, 2231−2243.
(53) Young, D. E.; McAchran, G. E.; Shore, S. G. *J. Am. Chem. Soc.* **1966**, *88*, 4390−4396.
(54) A minor quantity of $HB(NMe_2)_2$ (<1%) was also detected by ^{11}B NMR spectroscopy, with no observable change in the amount of residual amidodiborane **5** (which is present in samples of **1** − see discussion in text).
(55) Göttker-Schnetmann, I.; White, P. S.; Brookhart, M. *Organometallics* **2004**, *23*, 1766−1776.
(56) Vance, J. R.; Robertson, A. P. M.; Lee, K.; Manners, I. *Chem.—Eur. J.* **2011**, *17*, 4099−4103.
(57) The thermolyses of diborazanes **2** and **3** at 70 °C are much slower than that of **1** presumably due to presence of weaker terminal B−N bonds in the latter.
(58) Carpenter, J. D.; Ault, B. S. *J. Phys. Chem.* **1991**, *95*, 3507−3511.
(59) Pons, V.; Baker, R. T.; Szymczak, N. K.; Heldebrant, D. J.; Linehan, J. C.; Matus, M. H.; Grant, D. J.; Dixon, D. A. *Chem. Commun.* **2008**, 6597−6599.
(60) Chapman, A. M.; Haddow, M. F.; Wass, D. F. *J. Am. Chem. Soc.* **2011**, *133*, 8826−8829.
(61) Shrestha, R. P.; Diyabalanage, H. V. K.; Semelsberger, T. A.; Ott, K. C.; Burrell, A. K. *Int. J. Hydrogen Energy* **2009**, *34*, 2616−2621.
(62) In this case, $MeNH{=}BCy_2$ (**13**) could not be isolated cleanly for complete characterization. This was, however, achieved by performing an analogous experiment with $MeNH_2{-}BH_2{-}NHMe{-}BH_3$ (**3**) (see section (c)).
(63) If cyclohexene is used as the reaction solvent, thermolysis over 18 h at 70 °C leads to 33% $MeNH{=}BCy_2$ (**13**).
(64) The calibration and columns in our GPC system have a low molecular weight cut off at ca. 5000 g/mol, see experimental section (Supporting Information) for further details.
(65) Alcaraz, G.; Sabo-Etienne, S. *Angew. Chem., Int. Ed.* **2010**, *49*, 7170−7179.
(66) Vidovic, D.; Addy, D. A.; Kraemer, T.; McGrady, J.; Aldridge, S. *J. Am. Chem. Soc.* **2011**, *133*, 8494−8497.
(67) Alcaraz, G.; Chaplin, A. B.; Stevens, C. J.; Clot, E.; Vendier, L.; Weller, A. S.; Sabo-Etienne, S. *Organometallics* **2010**, *29*, 5591−5595.
(68) Chaplin, A. B.; Weller, A. S. *Inorg. Chem.* **2010**, *49*, 1111−1121.
(69) Tang, C. Y.; Thompson, A. L.; Aldridge, S. *Angew. Chem., Int. Ed.* **2010**, *49*, 921−925.
(70) Johnson, H. C.; Weller, A. S. *J. Organomet. Chem.* **2012**, *721−722*, 17−22.
(71) Alcaraz, G.; Vendier, L.; Clot, E.; Sabo-Etienne, S. *Angew. Chem., Int. Ed.* **2010**, *49*, 918−920.
(72) Tang, C. Y.; Thompson, A. L.; Aldridge, S. *J. Am. Chem. Soc.* **2010**, *132*, 10578−10591.
(73) Leitao, E. M.; Stubbs, N. E.; Robertson, A. P. M.; Helten, H.; Cox, R. J.; Lloyd-Jones, G. C.; Manners, I. *J. Am. Chem. Soc.* **2012**, *134*, 16805−16816.
(74) Pasumansky, L.; Haddenham, D.; Clary, J. W.; Fisher, G. B.; Goralski, C. T.; Singaram, B. *J. Org. Chem.* **2008**, *73*, 1898−1905.
(75) Products of diborazane component of the reaction: $[MeN{-}BH]_3$ (**12**) (9%), unreacted **2** (45%), amine-borane **8** (17%), amidoborane **5** (8%), and unknowns (21%) based on ^{11}B NMR spectroscopy.
(76) For detailed studies of the H_2 exchange in a model system based $Me_2NH{\cdot}BH_3$ (**7**) and $iPr_2N{=}BH_2$, see ref 73.

(77) Narula, C. K.; Janik, J. F.; Duesler, E. N.; Paine, R. T.; Schaeffer, R. *Inorg. Chem.* **1986**, *25*, 3346−3349.
(78) The catalysis studies of $MeNH_2$−BH_2−NHMe−BH_3 (**3**) were carried under conditions analogous to those employed in the polymerization of amine-borane **6** to enable a direct comparison. Experiments were also performed at 0.35 M and 1 mol % Ir loading, as for **1** and **2**, and indicated comparable behaviour although with a significantly reduced rate (see the Supporting Information for details).
(79) Although the ^{11}B NMR chemical shift of **6** is very similar to that of the terminal BH_3 group in **3** (δ_B = −19.3 ppm), toward the end of the reaction, the peak assigned to **6** appeared in the absence of that corresponding to the bridging environment of **3** (δ_B = −6.2 ppm [t, J_{BH} = 106 Hz]), reinforcing the assignment.
(80) The polymerization of $MeNH_2{\cdot}BH_3$ (**6**) with IrH_2POCOP in the presence of cyclohexene was also studied, producing no evidence of the formation of MeNH═BCy_2 (**13**), and the isolation of spectroscopically comparable $[MeNH\text{-}BH_2]_n$ (**16**) (see the Supporting Information for details).
(81) Jaska, C. A.; Lough, A. J.; Manners, I. *Inorg. Chem.* **2004**, *43*, 1090−1099.
(82) Ideally the mechanism could have been probed through selective deuterium labelling of the hydrides at boron in the terminal borane unit but synthetically this was found to be impossible to achieve (see the Supporting Information, section (v)).
(83) The composition of the solution did not change over the 24 h period and contained ∼4% **5** consistently throughout the time frame.
(84) This and all subsequent investigations of the thermal and catalytic redistribution of diborazane **1** were conducted in sealed J. Youngs NMR tubes in THF. The thermolyses were therefore carried out at 65 °C rather than the previously employed 70 °C to avoid significant pressure buildup.
(85) NEt_3 was selected as a model amine in place of Me_3N, due to the gaseous nature of the latter compound, which would have presented significant difficulties in the accurate addition of small quantities of reagent.
(86) Various redistribution pathways for diborazanes **1** and **3** were calculated using two computational methods B97D/6-31G(d,p) and PBE0/6-31(d,p), both in combination with the solvent model polarizable continuum model (PCM) for THF. For most reactions, the thermochemical data obtained with both methods were comparable. Therefore, only the data (free energies in solution at 65 °C) calculated with B97D/6-31(d,p) for diborazane **1** as a good case in point, are given in the main text (see the Supporting Information, section (iii) for complete results).
(87) *Mechanisms a* and *b* were also investigated by DFT methods, and were found to be unfavorable (see the Supporting Information).
(88) If a terminal N−H bond is present, as in diborazane **3**, the favored process is elimination of H_2 from the terminal N−H and B−H moieties, with concomitant cleavage of the central B−N bond and formation of two molecules of aminoborane **10** (see the Supporting Information).
(89) For previous calculations on the abstraction of BH_3 from μ-amidodiboranes by amines, see ref 73 and (a) Nutt, W. R.; McKee, M. L. *Inorg. Chem.* **2007**, *46*, 7633−7645. (b) Helten, H.; Robertson, A. P. M.; Staubitz, A.; Vance, J. R.; Haddow, M. F.; Manners, I. *Chem.—Eur. J.* **2012**, *18*, 4665−4680.
(90) Shimoi, M.; Nagai, S.-I.; Ichikawa, M.; Kawano, Y.; Katoh, K.; Uruichi, M.; Ogino, H. *J. Am. Chem. Soc.* **1999**, *121*, 11704−11712.